

## Supplementary of “New particle formation in marine atmosphere during seven cruise campaigns”

Yujiao Zhu<sup>1</sup>, Kai Li<sup>2</sup>, Yanjie Shen<sup>1</sup>, Yang Gao<sup>1</sup>, Xiaohuan Liu<sup>1</sup>, Yang Yu<sup>1</sup>, Huiwang Gao<sup>1</sup>, Xiaohong Yao<sup>1\*</sup>

<sup>1</sup>Key Lab of Marine Environmental Science and Ecology, Ministry of Education, Ocean University of China, Qingdao 266100, China

<sup>2</sup>National Marine Environmental Forecasting Center, Beijing, 100081, China

### List of Texts:

**Text S1** The chemical analysis of nano-MOUDI or MOUDI sample filters.

**Text S2** Calculations of new particle formation rate (FR), growth rate (GR) and condensation sink (CS).

### List of Figures:

**Figure S1** Satellite alue of NO<sub>2</sub> (GOME-2 observation) during November 2012 (a), May 2014 (b), August 2015 (c) and April 2014 (d).

**Figure S2** Comparison of N<sub><30 nm</sub> and D<sub>pg</sub> during four NPF days in 2012 (A: 14 October, B: 15 October, C: 17 October, D: 18 October).

**Figure S3** Seasonal variations of averaged particle size distributions over the marginal seas of China.

**Figure S4** Relationship between NMINP and FR, D<sub>pgmax</sub> and GR in NPF events occurred in the coastal atmosphere.

**Figure S5** Figure S5 24-h air mass back trajectories on NPF days from 2012 to 2015 (red lines represent that of the location of ship, blue lines represent that of the location of OUC).

**Figure S6** MODIS derived chlorophyll-a oceanic concentrations averaging from 8 April and 13 April, 2014.

### List of Tables:

**Table S1** Comparison of same NPF events measured by FMPS and SMPS.

**Text S1** The chemical analysis of nano-MOUDI or MOUDI sample filters.

The collected samples were wrapped with baked aluminum foils (pre-combusted at 450°C for 6 h in a furnace to eliminate the absorbed organic compounds) and sealed in polyethylene bags, then stored in darkness at -20°C before chemical analysis. All samples were ultrasonically extracted in deionized water (18.2 M Ω • cm) for 20 min at 0°C. The mass concentrations of sodium (Na<sup>+</sup>), ammonium (NH<sub>4</sub><sup>+</sup>), potassium (K<sup>+</sup>), magnesium (Mg<sup>2+</sup>), calcium (Ca<sup>2+</sup>), dimethylammonium (DMA<sup>+</sup>), trimethylammonium (TMA<sup>+</sup>), chloride (Cl<sup>-</sup>), nitrite (NO<sub>2</sub><sup>-</sup>), nitrate (NO<sub>3</sub><sup>-</sup>), sulfate (SO<sub>4</sub><sup>2-</sup>), phosphate (PO<sub>4</sub><sup>3-</sup>), formate (HCO<sub>2</sub><sup>-</sup>), acetate (C<sub>2</sub>H<sub>3</sub>O<sub>2</sub><sup>-</sup>), oxalate (C<sub>2</sub>O<sub>4</sub><sup>2-</sup>) and succinate (C<sub>4</sub>H<sub>4</sub>O<sub>4</sub><sup>2-</sup>) were determined using Dionex ICS-3000 and Dionex ICS-1100 ion chromatographs equipped with different analytic columns. The QA/QC was detailed in Hu et al. (2015). All results were corrected with field blanks.

**Text S2** Calculations of new particle formation rate (FR), growth rate (GR) and condensation sink (CS).

The formation rate of new particles (FR), taking consideration of the coagulation and growth losses, was calculated using the method provided by Sihto et al., (2006):

$$FR = \frac{dN_{dp}}{dt} + CoagS_{dp} \cdot N_{dp} + \frac{GR}{\Delta d_p} \cdot N_{dp} + S_{losses} \quad (1)$$

where  $d_p$  is the sizes of nucleation mode particles. For FMPS, it is denoted by 5.6-30 nm particles, while for SMPS, it is denoted by 10-30 nm particles.  $N_{dp}$  is the particle number concentration of nucleation mode particles. The coagulation loss for particles ( $CoagS_{dp} \cdot N_{dp}$ ) was the sum of particle-particle inter- and hetero-coagulation rates. The growth loss ( $GR/\Delta d_p \cdot N_{dp}$ ) is due to condensation growth out of the nucleation mode sizes during the calculation period.  $S_{losses}$  includes additional losses and is assumed to be zero.

The apparent growth rate (GR) of new particles was calculated by:

$$GR = \frac{\Delta D_{pg}}{\Delta t} \quad (2)$$

where  $D_{pg}$  was fitted by the multiple log-normal distribution functions (Whitby, 1978; Zhu et al., 2014), and  $\Delta t$  was the duration for the growth of new particles.

The condensation sink (CS) is the loss rate of condensable vapor molecules onto the pre-existing particles, and calculated as Kulmala et al. (2001, 2005) and Dal Maso et al. (2005):

$$CS = 2\pi D \int D_p \beta_M(D_p) n(D_p) dD_p = 2\pi D \sum_i \beta_{Mi} D_{pi} N_{pi} \quad (3)$$

where  $D$  is the diffusion coefficient,  $\beta_M$  is the transitional regime correction factor,  $D_{pi}$  is the particle diameter of size class  $i$ , and  $N_{pi}$  is the particle number concentration in size class  $i$ .

## References

- Dal Maso, M., Kulmala, M., Riipinen, I., Wagner, R., Hussein, T., Aalto, P. P., and Lehtinen, K. E. J.: Formation and growth of fresh atmospheric aerosols: Eight years of aerosol size distribution data from SMEAR II, Hyytiälä, Finland, *Boreal Environ. Res.* 10, 323-336, 2005.
- Hu, Q., Yu, P., Zhu, Y., Li, K., Gao, H., and Yao, X. Concentration, size distribution, and formation of trimethylammonium and dimethylammonium ions in atmospheric particles over marginal seas of China, *J. Atmos. Sci.*, 72, 3487-3498, doi:10.1175/JAS-D-14-0393.1, 2015.
- Kulmala, M., Dal Maso, M., Mäkelä, J. M., Pirjola, L., Väkevä, M., Aalto, P., Miikkulainen, P., Hämeri, K., and O'Dowd, C. D.: On the formation, growth and composition of nucleation mode particles, *Tellus B*, 53, 479-490, doi:10.1034/j.1600-0889.2001.530411.x, 2001.
- Kulmala, M., Petäjä, T., Mönkkönen, P., Koponen, I.K., Dal Maso, M., Aalto, P. P., Lehtinen, K. E. J., and Kerminen, V. M.: On the growth of nucleation mode particles: Source rates of condensable vapor in polluted and clean environments. *Atmos. Chem. Phys.*, 5, 409-416, doi:10.5194/acp-5-409-2005, 2005.
- Sihto, S.-L., Kulmala, M., Kerminen, V.-M., Dal Maso, M., Petäjä, T., Riipinen, I., Korhonen, H., Arnold, F., Janson, R., Boy, M., Laaksonen, A., and Lehtinen, K. E. J.: Atmospheric sulphuric acid and aerosol formation: implications from atmospheric measurements for nucleation and early growth mechanisms, *Atmos. Chem. Phys.*, 6, 4079–4091, doi:10.5194/acp-6-4079-2006, 2006.
- Whitby, K. T.: The physical characteristics of sulfur aerosols, *Atmos. Environ.*, 12, 135-159, doi:10.1016/0004-6981(78)90196-8, 1978.
- Zhu, Y., Sabaliauskas, K., Liu, X., Meng, H., Gao, H., Jeong, C. H., Evans, G. J., and Yao, X.: Comparative analysis of new particle formation events in less and severely polluted urban atmosphere, *Atmos. Environ.*, 98, 655-664, doi:10.1016/j.atmosenv.2014.09.043, 2014.

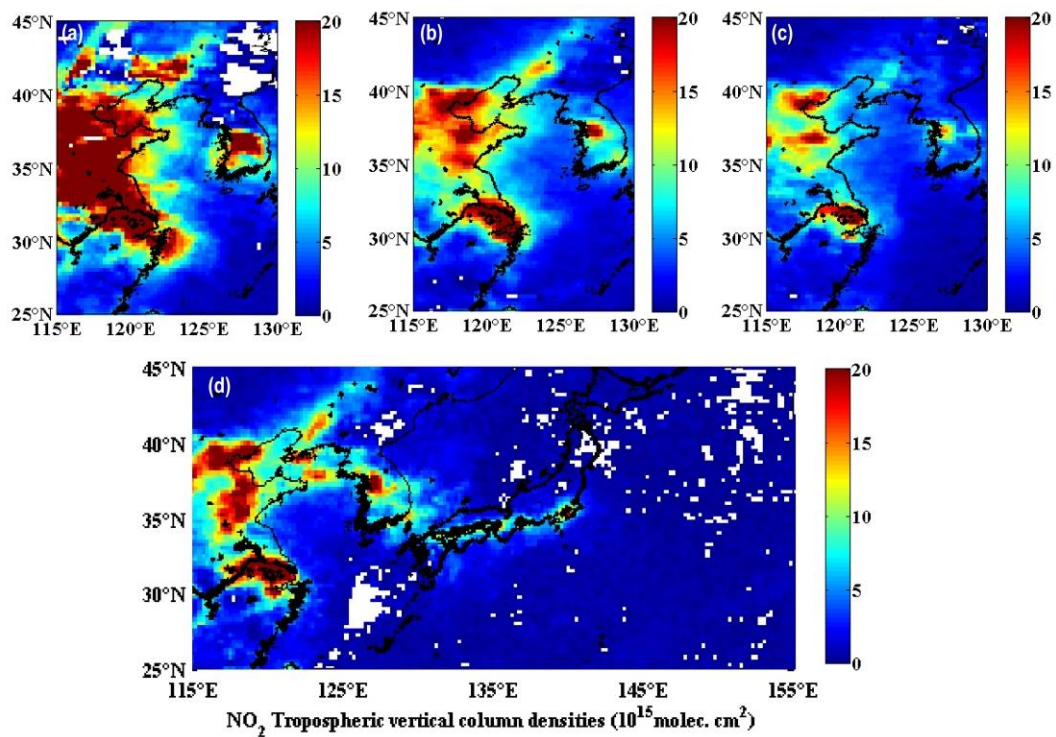


Figure S1 Satellite value of  $\text{NO}_2$  (GOME-2 observation) during November 2012 (a), May 2014 (b), August 2015 (c) and April 2014 (d).

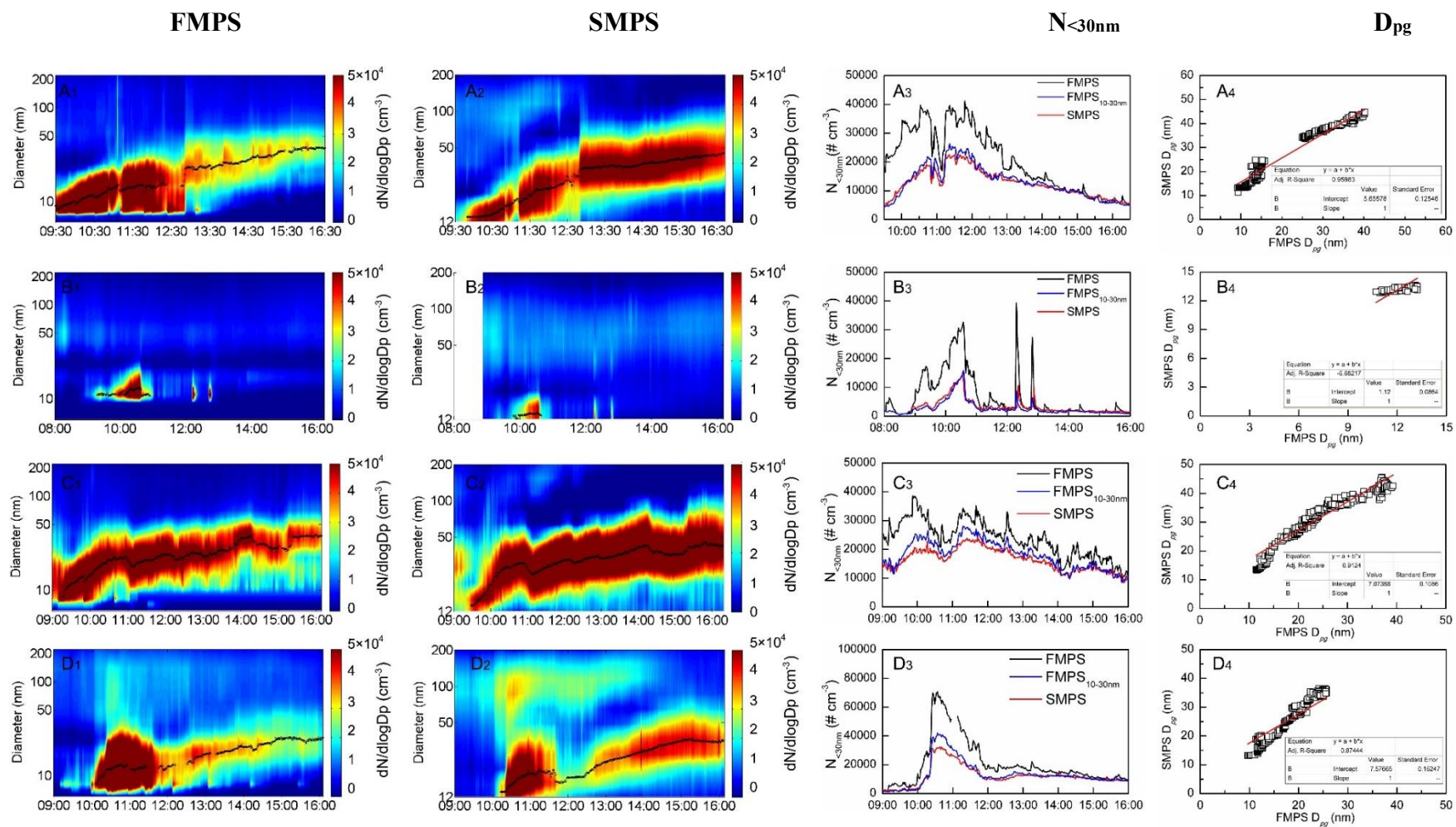


Figure S2 Comparison of  $N_{<30\text{ nm}}$  and  $D_{pg}$  during four NPF days in 2012 (A: 14 October, B: 15 October, C: 17 October, D: 18 October).

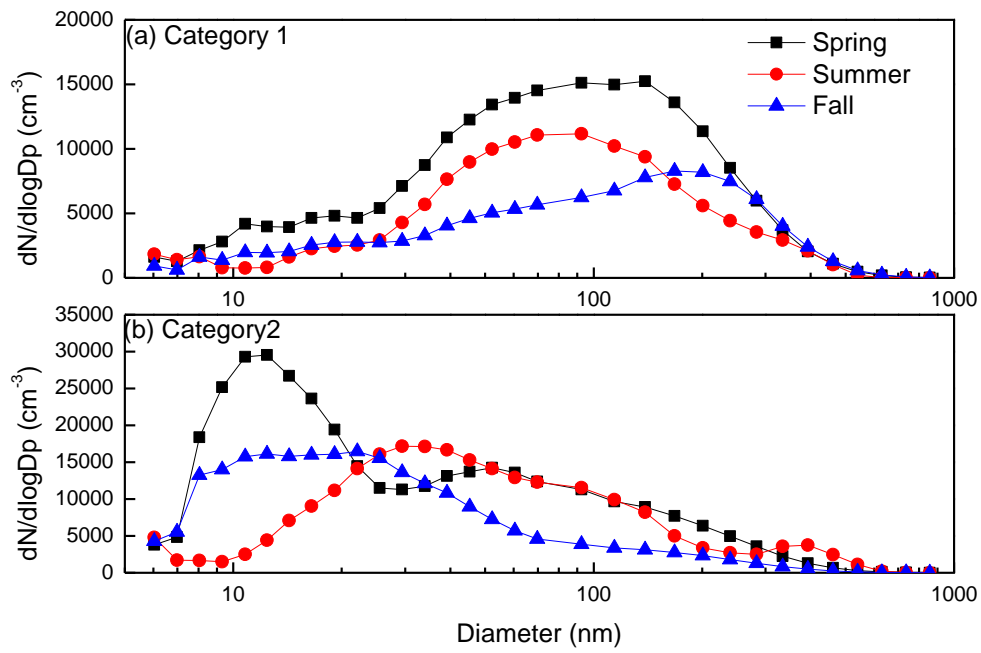


Figure S3 Seasonal variations of averaged particle size distributions over the marginal seas of China.

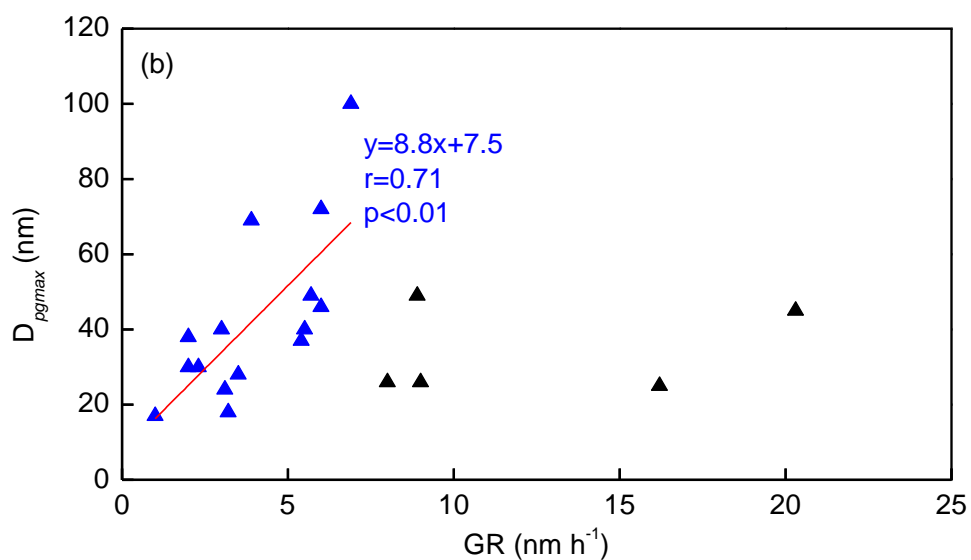
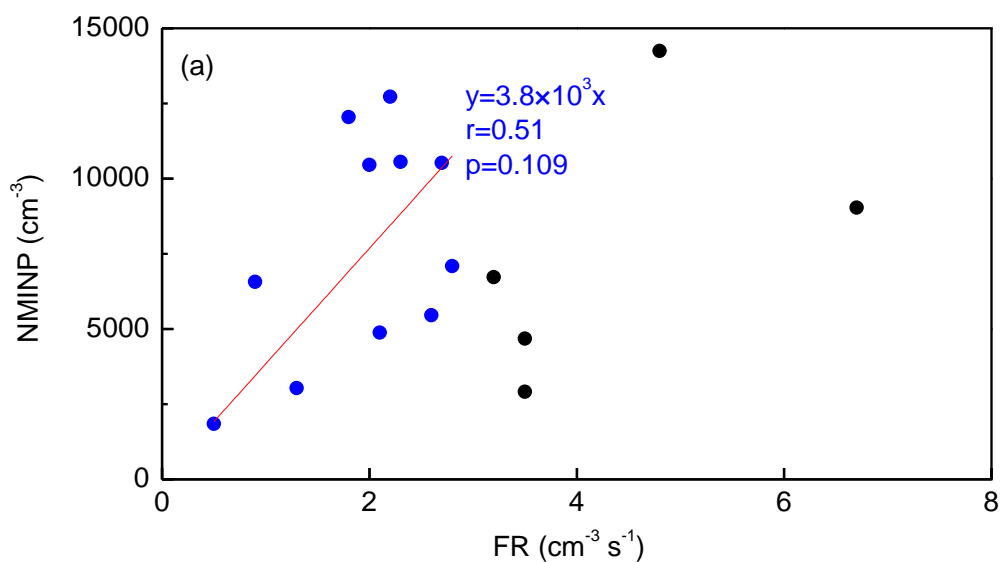
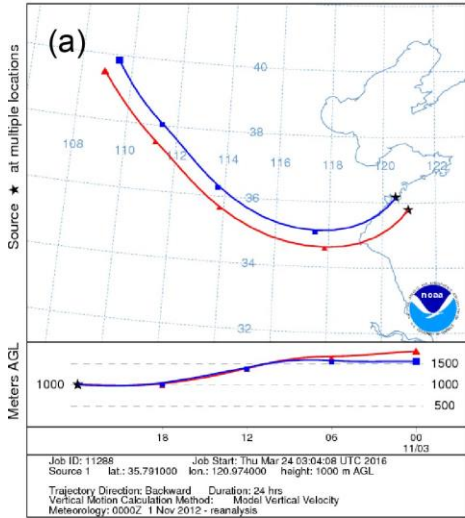
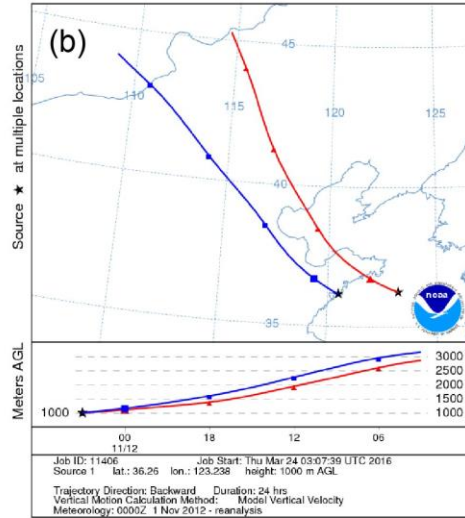


Figure S4 Relationship between net maximum increase in nucleation mode particles number concentration (NMINP) and new particle formation rate (FR), maximum geometric median diameter of new particles ( $D_{pgmax}$ ) and growth rate (GR) in NPF events occurred at OUC site (Black symbols were treated as exteriors and excluded from the correlation analysis).

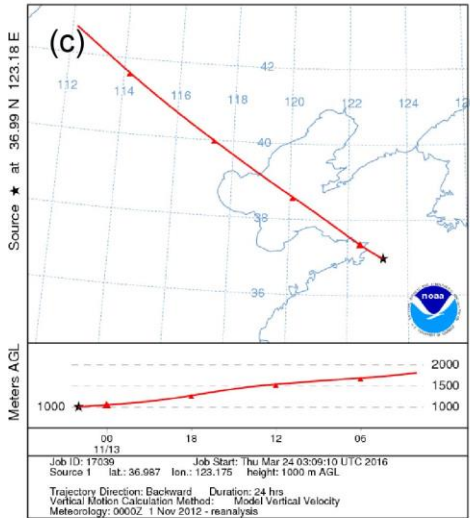
NOAA HYSPLIT MODEL  
Backward trajectories ending at 0000 UTC 04 Nov 12  
CDC1 Meteorological Data



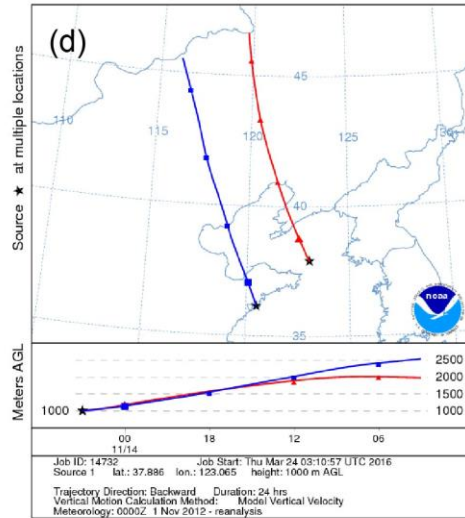
NOAA HYSPLIT MODEL  
Backward trajectories ending at 0300 UTC 12 Nov 12  
CDC1 Meteorological Data



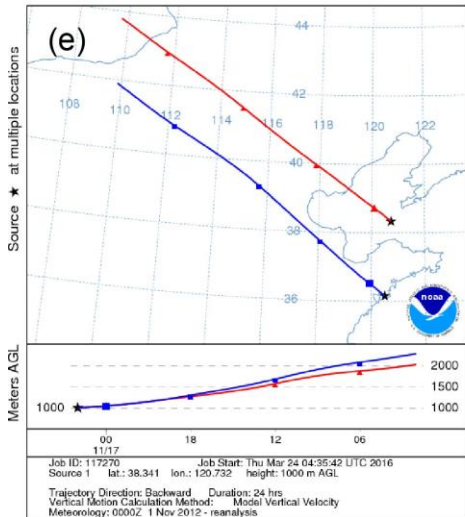
NOAA HYSPLIT MODEL  
Backward trajectory ending at 0200 UTC 13 Nov 12  
CDC1 Meteorological Data



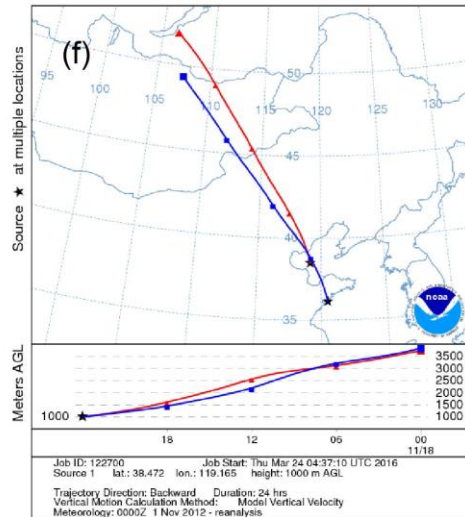
NOAA HYSPLIT MODEL  
Backward trajectories ending at 0300 UTC 14 Nov 12  
CDC1 Meteorological Data



NOAA HYSPLIT MODEL  
Backward trajectories ending at 0200 UTC 17 Nov 12  
CDC1 Meteorological Data

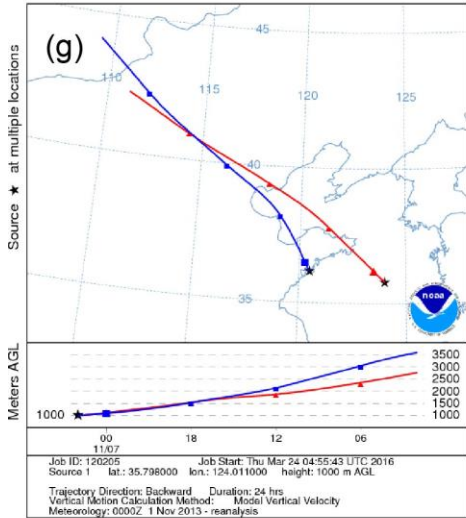


NOAA HYSPLIT MODEL  
Backward trajectories ending at 0000 UTC 19 Nov 12  
CDC1 Meteorological Data

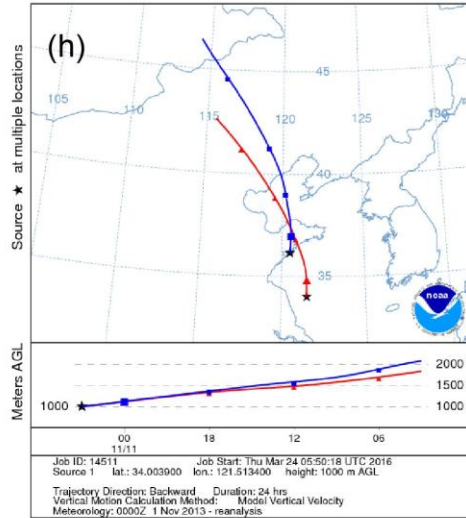




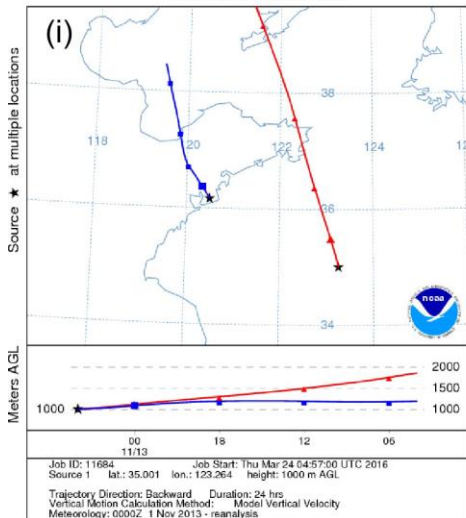
NOAA HYSPLIT MODEL  
Backward trajectories ending at 0200 UTC 07 Nov 13  
CDC1 Meteorological Data



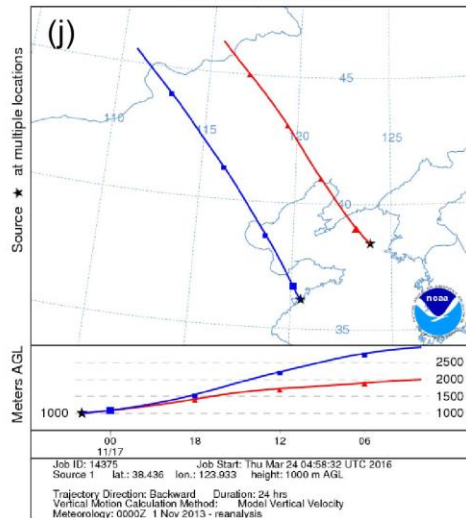
NOAA HYSPLIT MODEL  
Backward trajectories ending at 0300 UTC 11 Nov 13  
CDC1 Meteorological Data



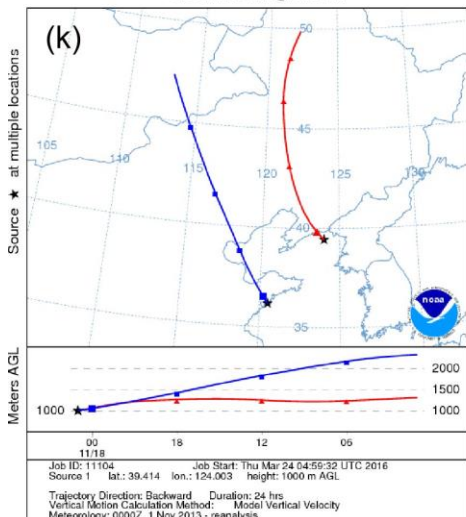
NOAA HYSPLIT MODEL  
Backward trajectories ending at 0400 UTC 13 Nov 13  
CDC1 Meteorological Data



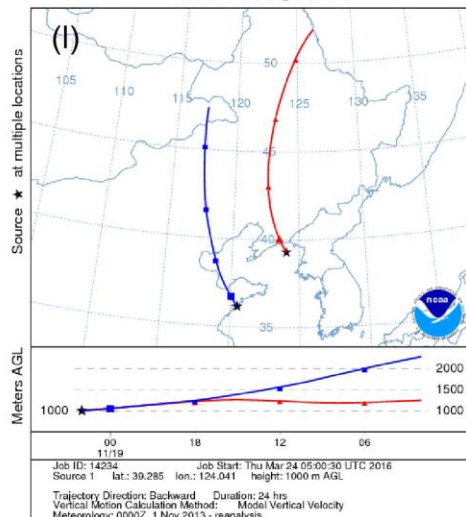
NOAA HYSPLIT MODEL  
Backward trajectories ending at 0200 UTC 17 Nov 13  
CDC1 Meteorological Data



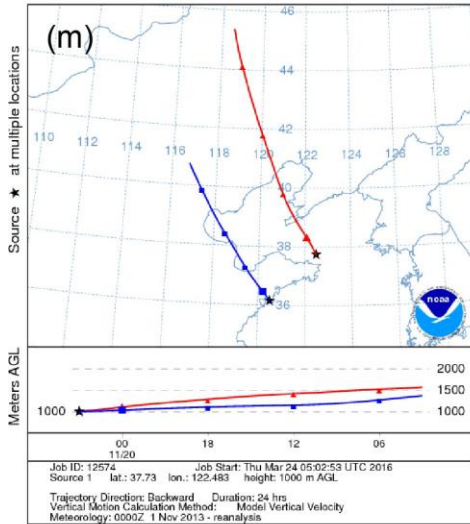
NOAA HYSPLIT MODEL  
Backward trajectories ending at 0100 UTC 18 Nov 13  
CDC1 Meteorological Data



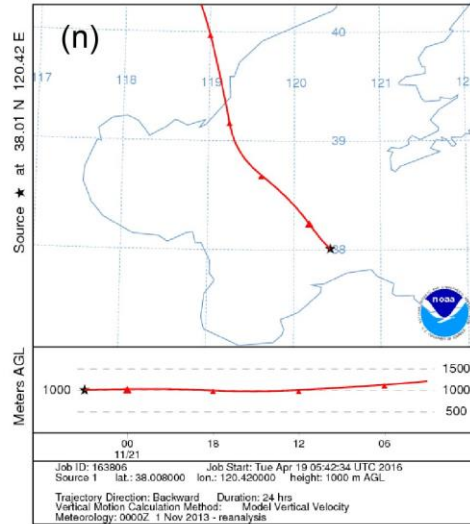
NOAA HYSPLIT MODEL  
Backward trajectories ending at 0200 UTC 19 Nov 13  
CDC1 Meteorological Data



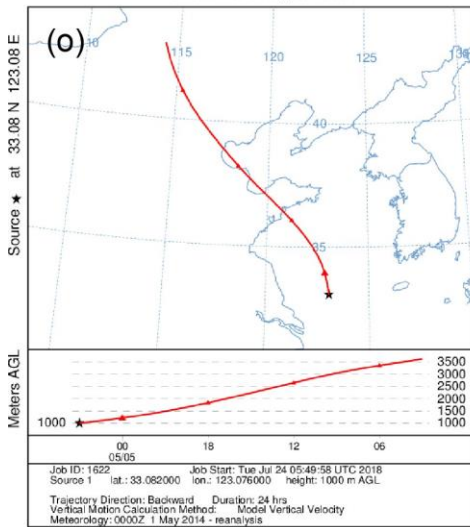
NOAA HYSPLIT MODEL  
Backward trajectories ending at 0300 UTC 20 Nov 13  
CDC1 Meteorological Data



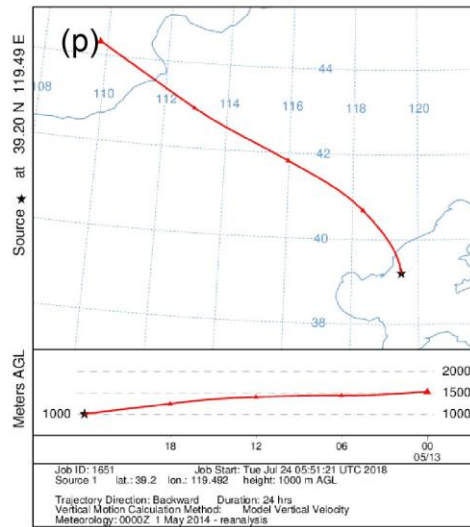
NOAA HYSPLIT MODEL  
Backward trajectory ending at 0300 UTC 21 Nov 13  
CDC1 Meteorological Data



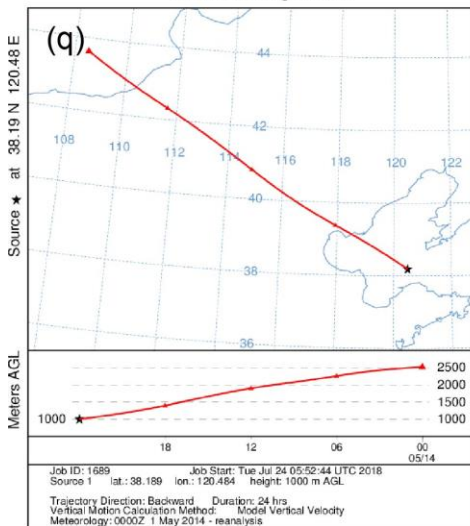
NOAA HYSPLIT MODEL  
Backward trajectory ending at 0300 UTC 05 May 14  
CDC1 Meteorological Data



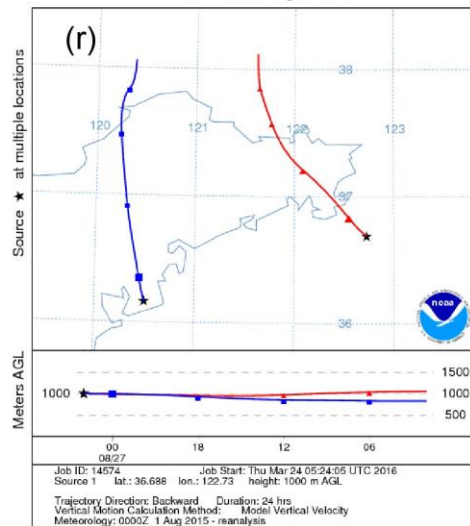
NOAA HYSPLIT MODEL  
Backward trajectory ending at 0000 UTC 14 May 14  
CDC1 Meteorological Data



NOAA HYSPLIT MODEL  
Backward trajectory ending at 0000 UTC 15 May 14  
CDC1 Meteorological Data



NOAA HYSPLIT MODEL  
Backward trajectories ending at 0200 UTC 27 Aug 15  
CDC1 Meteorological Data



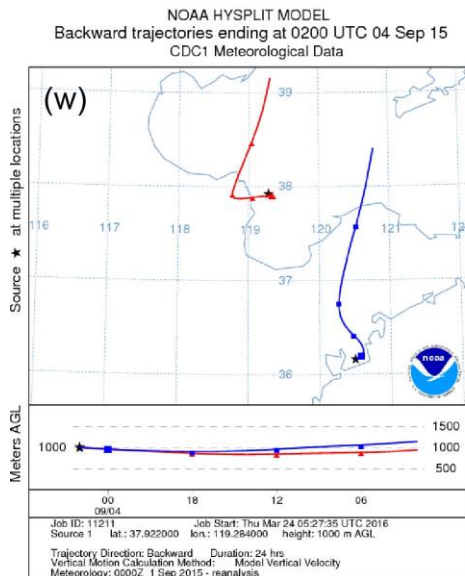
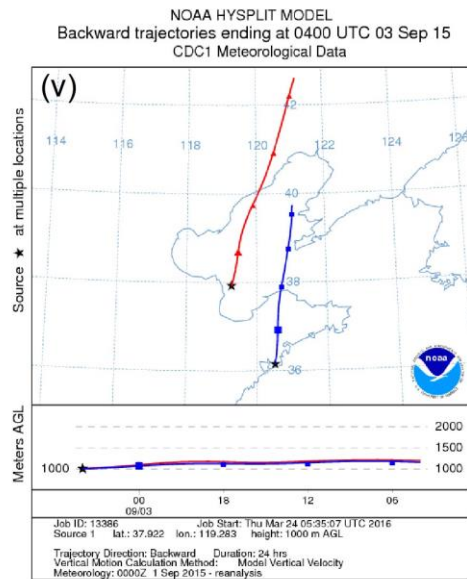
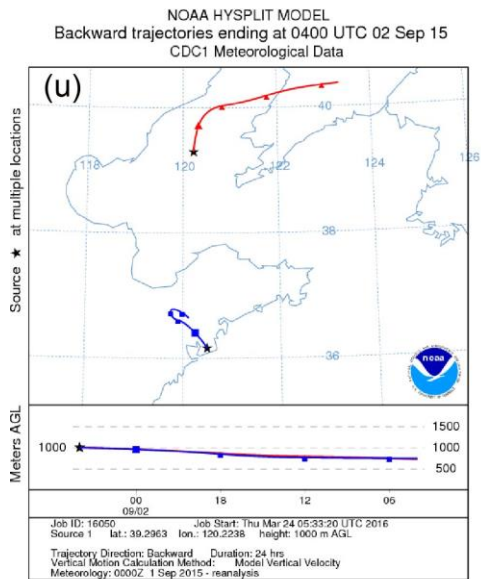
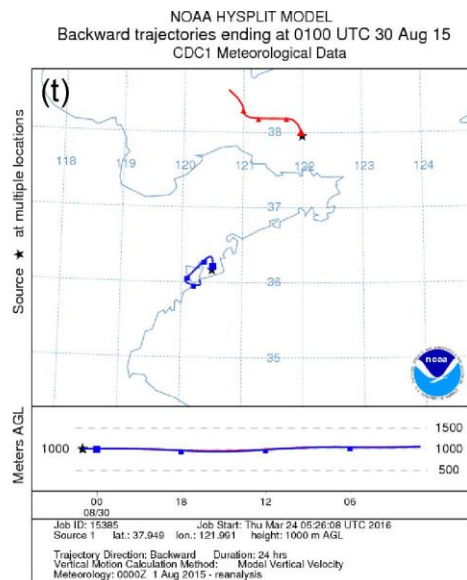
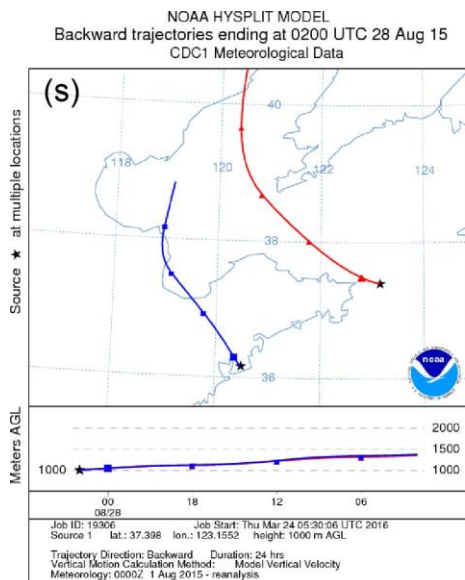


Figure S5 24-h air mass back trajectories on NPF days from 2012 to 2015 (red lines represent that of the location of ship, blue lines represent that of the location of OUC).

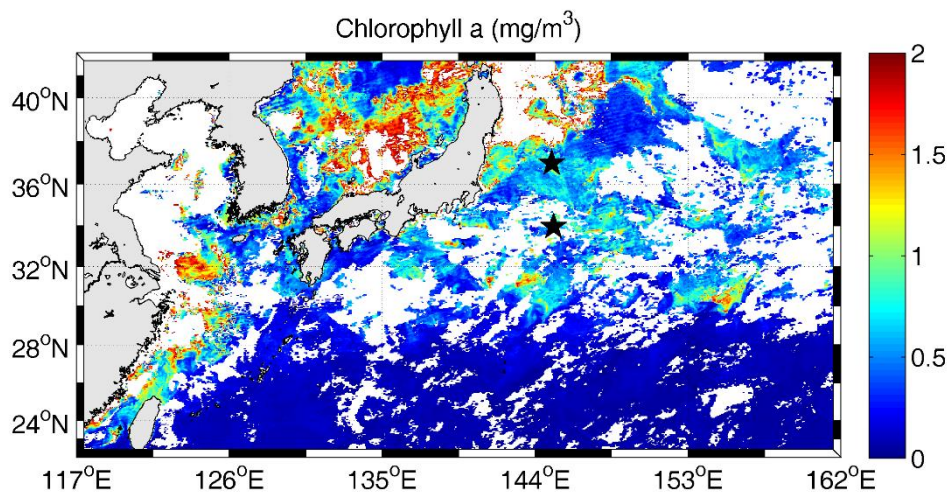


Figure S6 MODIS derived chlorophyll-a oceanic concentrations averaging from 8 April and 13 April, 2014.

Table S1 Comparison of same NPF events measured by FMPS and SMPS.

		FR (particles cm <sup>-3</sup> )	GR (nm h <sup>-1</sup> )
14 October	FMPS	8.4	4.7
	FMPS <sub>10-30nm</sub>	8.4	4.7
	SMPS	6.8	5
15 October	FMPS	7.3	
	FMPS <sub>10-30nm</sub>	4.7	
	SMPS	4.2	
17 October	FMPS	6.8	3.7
	FMPS <sub>10-30nm</sub>	6.8	3.7
	SMPS	6.2	4.5
18 October	FMPS	39.3	3.8
	FMPS <sub>10-30nm</sub>	25.9	3.8
	SMPS	21.8	4.7